

# Characterizations of the hydrogen-bond structures of 2-naphthol-(H<sub>2</sub>O)<sub>n</sub> (n = 0-3 and 5) clusters by infrared-ultraviolet double-resonance spectroscopy

著者	三上 直彦
journal or publication title	Journal of chemical physics
volume	109
number	15
page range	6303-6311
year	1998
URL	<a href="http://hdl.handle.net/10097/35707">http://hdl.handle.net/10097/35707</a>

doi: 10.1063/1.477272

# Characterizations of the hydrogen-bond structures of 2-naphthol-(H<sub>2</sub>O)<sub>n</sub> (*n*=0–3 and 5) clusters by infrared-ultraviolet double-resonance spectroscopy

Yoshiteru Matsumoto, Takayuki Ebata, and Naohiko Mikami

*Department of Chemistry, Graduate School of Science, Tohoku University, Sendai 980-8578, Japan*

(Received 1 May 1998; accepted 13 July 1998)

OH stretching vibrations of 2-naphthol-(H<sub>2</sub>O)<sub>n</sub> (*n*=0–3 and 5) hydrogen-bonded clusters in the *S*<sub>0</sub> state have been observed by infrared-ultraviolet (IR-UV) double-resonance spectroscopy. In bare 2-naphthol, *cis*- and *trans*-isomers were identified by the comparison of the observed OH frequencies with those obtained by *ab initio* calculations with the HF/6-31G basis set. The OH stretching vibrations ( $\nu_{\text{OH}}$ ) of hydrogen-bonded 2-naphthol-(H<sub>2</sub>O)<sub>n</sub> show characteristic shifts depending on the cluster size. They are classified into hydrogen-bonded  $\nu_{\text{OH}}$ , and  $\nu_{\text{OH}}$  free from the hydrogen bond. The cluster structures were also examined by comparing the observed IR spectra with simulated ones. It was found that the clusters with *n*=2 and 3 form ring structures, while the cluster with *n*=5 exhibits an ice (*I*) structure. © 1998 American Institute of Physics.  
[S0021-9606(98)00239-6]

## I. INTRODUCTION

Hydrogen-bonded (H-bonded) clusters between aromatic acids and water molecules, generated in supersonic jets, have been of considerable interest for many years. Among them, phenol-(H<sub>2</sub>O)<sub>n</sub>, 1- and 2-naphthol-(H<sub>2</sub>O)<sub>n</sub> clusters have been thought to give a basic idea for the structures and dynamics of the H-bonded system of aromatic molecules.<sup>1–19</sup> Most of the studies have been done so far by the use of electronic spectroscopy, such as resonance enhanced multiphoton ionization (REMPI) with mass-selection, laser induced fluorescence (LIF), dispersed fluorescence, and stimulated emission pumping techniques.<sup>1–19</sup> High resolution electronic spectroscopy and rotational coherence spectroscopy have been also applied to obtain their rotational constants.<sup>20,21</sup>

Recently, several vibrational spectroscopic studies using a double-resonance technique have been successfully applied to observe the OH stretching vibrations which provide the key feature of the H-bonds. The observation of the OH stretching vibration of a jet-cooled aromatic molecule and its clusters was first reported by Felker and co-workers, who applied stimulated Raman-UV double-resonance spectroscopy or ionization-detected stimulated Raman spectroscopy (IDSRS) to the H-bonded clusters of phenol.<sup>22</sup> In this spectroscopy, the population depletion of the ground vibrational level induced by stimulated Raman pumping is monitored by resonance enhanced multiphoton ionization (REMPI) with an ultraviolet (UV) laser. Our group applied a similar double-resonance method by using an infrared (IR) light source, IR-UV double-resonance spectroscopy, for the observation of the OH vibrational level. Here, a depletion of the ground state population by an effective vibrational excitation with the IR light is monitored by an electronic transition with the UV light. IR-UV double-resonance spectroscopy has been successfully applied by several groups to the H-bonded clusters, such as (phenol)<sub>n</sub>,<sup>23</sup> phenol-(H<sub>2</sub>O)<sub>n</sub>,<sup>24–26</sup>

phenol-amines,<sup>27</sup> and tropolone-(H<sub>2</sub>O)<sub>n</sub> and tropolone-(CH<sub>3</sub>OH)<sub>n</sub>.<sup>28–30</sup> For phenol-(H<sub>2</sub>O)<sub>n=1–5</sub>, for example, the OH stretching vibrations of the phenol site as well as H<sub>2</sub>O sites were observed and the cluster structures were determined by comparing the observed IR spectra with those obtained by *ab initio* calculations.<sup>26,31</sup>

In the present paper, we report the spectroscopic investigation of the OH stretching vibrations and the structures of the 2-naphthol-(H<sub>2</sub>O)<sub>n</sub> clusters in the *S*<sub>0</sub> state. It is known that the acidity of 2-naphthol increases drastically upon electronic excitation, and the dynamics of the H-bonded clusters of electronically excited 2-naphthol, including the proton transfer reaction with polar solvents, has been studied by several groups. For the 2-naphthol-(H<sub>2</sub>O)<sub>n</sub> clusters, the LIF and dispersed fluorescence spectra have been reported.<sup>16,19</sup> However, detailed information about the H-bonding structures of the 2-naphthol-(H<sub>2</sub>O)<sub>n</sub> clusters could not be provided from the analyses of electronic spectroscopy alone. In this work, we characterize the H-bond structures of 2-naphthol-(H<sub>2</sub>O)<sub>n</sub> clusters on the basis of the analysis of the observed IR spectra of the OH stretching vibrations with the help of *ab initio* calculations. For 2-naphthol-(H<sub>2</sub>O)<sub>n</sub> clusters, there are several interesting points; the first is that there are two rotamers, *cis*- and *trans*-forms in 2-naphthol. It may be possible to distinguish two rotamers by the difference of their OH stretching vibrational frequencies. The second point is whether we can see any differences in cluster structures between *cis*- and *trans*-forms, and what would be a major reason for the difference, if any. The third point is the comparison of the IR spectra of 2-naphthol-(H<sub>2</sub>O)<sub>n</sub> with those of phenol-(H<sub>2</sub>O)<sub>n</sub>. The pK<sub>a</sub> value of 2-naphthol in *S*<sub>0</sub> is 9.45,<sup>32,33</sup> which is slightly smaller than that of phenol (pK<sub>a</sub>=9.82); the difference in pK<sub>a</sub> will be expected to affect the hydrogen bond of the clusters.

## II. EXPERIMENT

In the present experiment, we applied fluorescence detected infrared spectroscopy (FDIRS) for the observation of

the vibrational spectrum of size-selected 2-naphthol-(H<sub>2</sub>O)<sub>n</sub> clusters. The experimental setup for FDIRS was the same as that described elsewhere.<sup>25</sup> A brief description will be given in the following. The 2-naphthol-(H<sub>2</sub>O)<sub>n</sub> clusters were generated by a supersonic expansion of a gaseous mixture of 2-naphthol and H<sub>2</sub>O, which is seeded in He. 2-naphthol was heated at 350 K to obtain sufficient vapor pressure. The mixture was expanded into a vacuum chamber through a pulsed valve having an 800 μm orifice.

The tunable UV and IR laser beams were introduced coaxially in opposite directions into the vacuum chamber. They were focused on the supersonic free jet at 15 mm downstream of the nozzle by using lenses (an  $f=500$  mm lens for UV and an  $f=250$  mm CaF<sub>2</sub> lens for IR). The IR laser pulse was introduced 50 ns prior to the UV laser pulse, which was controlled with a digital delay generator (SRS DG535). The frequency of the UV laser light was fixed to the  $S_1-S_0$  electronic transition, normally the 0-0 band, of a specific cluster, and its fluorescence intensity was monitored. When the IR laser frequency is resonant with the vibrational transition of the cluster, the ground state population is pumped to the vibrationally excited state, resulting in depletion of the fluorescence signal. Thus, FDIR spectra were obtained by scanning the IR laser frequency while monitoring the fluorescence signal.

The UV source was a second harmonic of a XeCl excimer laser pumped dye laser (Lambda Physik LPX100/FL2002). The pulse energy and the spectral resolution of the UV laser were 5 μJ and 0.2 cm<sup>-1</sup>, respectively. Fluorescence was collected by a lens and detected by a photomultiplier tube (Hamamatsu Photonics 1P28). The photocurrent from the photomultiplier tube was integrated by a boxcar integrator (Par Model 4400/4402) connected with a microcomputer. Tunable IR laser pulse was generated by a difference-frequency mixing between a second harmonic of an injection seeded Nd:YAG laser (Quanta Ray GCR 230) and a Nd:YAG laser pumped dye laser (Continuum ND6000, DCM dye) with a LiNbO<sub>3</sub> crystal. The pulse energy and the spectral resolution of the IR laser were 0.4 mJ and 0.1 cm<sup>-1</sup>, respectively. The lasers and the pulsed valve were operated with a repetition of 10 Hz.

In the present study, we also applied mass-selected REMPI spectroscopy to specify the size of each cluster in the electronic spectra. The experimental setup for this spectroscopy was described previously.<sup>34</sup> Briefly, the cluster ions generated by the REMPI were mass selected by a quadrupole mass filter and detected by an electron multiplier. The ion current was amplified by a current amplifier and averaged by a digital boxcar integrator system.

2-naphthol was purchased from Wako Chemical Industries, Ltd. and purified by vacuum sublimation before used.

To analyze the structures and the vibrational spectra of 2-naphthol-(H<sub>2</sub>O)<sub>n</sub>, *ab initio* molecular orbital calculations were performed. The energy-optimized structures and harmonic vibrational frequencies, as well as their IR intensities, were obtained at the HF/6-31G level. According to the calculation done by Watanabe and Iwata,<sup>31</sup> the calculation at the HF/6-31G level did not provide precise relative energies of isomers of the H-bonded clusters of phenol. However, they

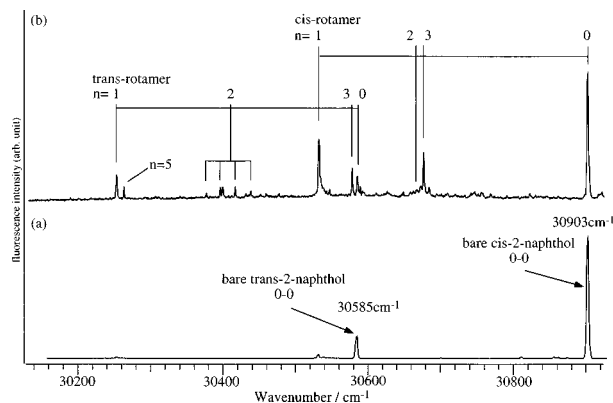


FIG. 1. Laser induced fluorescence (LIF) spectra of 2-naphthol and 2-naphthol-(H<sub>2</sub>O)<sub>n</sub> clusters measured under (a) low concentration, and (b) high concentration of water vapor.

showed that for the calculation of the IR spectra in the  $\nu_{OH}$  region, this level was enough to reproduce the observed spectra. Since we determine the structures of the clusters by the comparison of the vibrational spectra in the  $\nu_{OH}$  region in the present work, the calculation with this level is thought to give reliable results. The calculated frequencies of the  $\nu_{OH}$  vibrations were adjusted by multiplying a scaling factor of 0.9034. This scaling factor is determined so as to fit the calculated  $\nu_{OH}$  frequency of *cis*-rotamer to the observed one, and this factor is also used for all the clusters. The program used was GAUSSIAN 92.<sup>35</sup>

### III. RESULTS AND DISCUSSION

#### A. $S_1-S_0$ electronic spectra of 2-naphthol and 2-naphthol-(H<sub>2</sub>O)<sub>n</sub>

Figure 1(a) shows the  $S_1-S_0$  LIF spectrum of 2-naphthol measured under a condition of a low water vapor pressure. The spectrum is essentially the same as that reported by Oikawa and others, who emphasized the discrimination of the two rotamers in the electronic spectrum.<sup>36</sup> According to the recent assignment given by Johnson and co-workers, who observed the rotationally resolved LIF spectrum,<sup>37</sup> two prominent peaks at 30 903 and 30 585 cm<sup>-1</sup> are assigned to the origin bands of *cis*- and *trans*-rotamers of bare 2-naphthol, respectively. In the present work, as will be discussed below, we confirmed their assignment for the two rotamers by comparing the IR spectra of the OH stretching vibrations with those obtained by *ab initio* calculations.

Figure 1(b) shows the  $S_1-S_0$  LIF spectrum of 2-naphthol measured under a higher H<sub>2</sub>O vapor pressure condition, so that many bands due to the clusters with H<sub>2</sub>O were observed. The bands of each cluster were assigned from the results of the mass-selected REMPI spectra and the analysis of the IR spectra described later. Figures 2(b)–2(e) show the mass-selected REMPI spectra, which are compared with the LIF spectrum of Fig. 2(a). Since the  $S_1-S_0$  transition energy of bare 2-naphthol is less than a half of the ionization potential (63 670 for *cis*-rotamer and 63 189 cm<sup>-1</sup> for *trans*-rotamer),<sup>38</sup> its multiphoton ionization (MPI) spectrum [Fig. 2(b)] was measured by two-color (1+1') REMPI with  $h\nu_2=34\,000$  cm<sup>-1</sup>. Figure 2(b) shows the REMPI spectrum

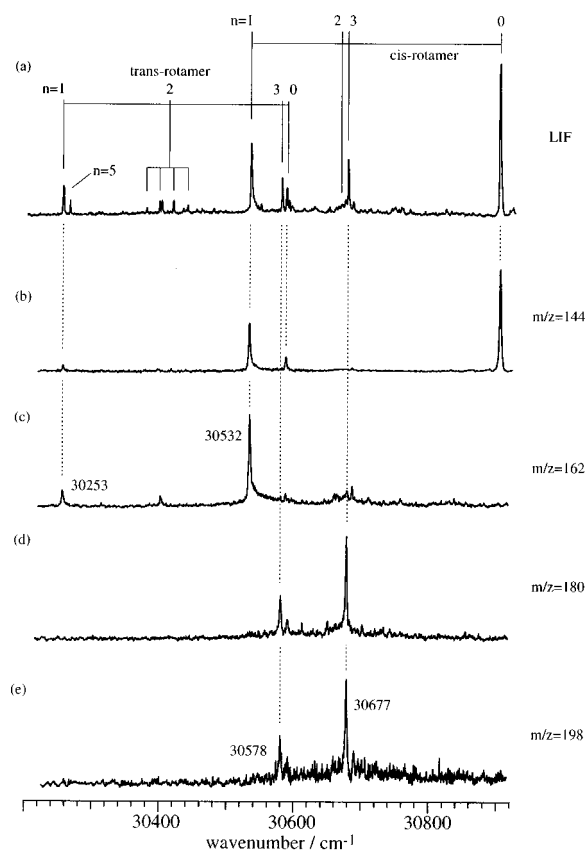


FIG. 2. (a) LIF spectrum of 2-naphthol-(H<sub>2</sub>O)<sub>n</sub>, same as Fig. 1(b). (b)–(e) mass-selected REMPI spectra of 2-naphthol-(H<sub>2</sub>O)<sub>n</sub>: the monitoring masses are (b)  $m/z=144$ , [naphthol]<sup>+</sup>, (c)  $m/z=162$ , [naphthol-H<sub>2</sub>O]<sup>+</sup>, (d)  $m/z=180$ , [naphthol-(H<sub>2</sub>O)<sub>2</sub>]<sup>+</sup>, (e)  $m/z=198$ , [naphthol-(H<sub>2</sub>O)<sub>3</sub>]<sup>+</sup>, respectively. The spectrum (b) was measured by two-color (1+1') REMPI with  $h\nu_2=34\,000\text{ cm}^{-1}$ .

obtained by monitoring [naphthol]<sup>+</sup> ( $m/z=144$ ). In this spectrum, besides the bands of bare *cis*- and *trans*-2-naphthol, two bands are observed at 30 532 and 30 253  $\text{cm}^{-1}$ . Since these bands are observed at the  $m/z=162$  (corresponding to [naphthol-H<sub>2</sub>O]<sup>+</sup>), but not at the mass of  $m/z=180$  (corresponding to [naphthol-(H<sub>2</sub>O)<sub>2</sub>]<sup>+</sup>), they are assigned to the 0-0 bands of *cis*- and *trans*-2-naphthol-H<sub>2</sub>O clusters, respectively. In a similar manner, we identified the cluster size by measuring the mass-selected REMPI spectrum. In general, two ion products were observed for each cluster, that is [naphthol-(H<sub>2</sub>O)<sub>n</sub>]<sup>+</sup> and [naphthol-(H<sub>2</sub>O)<sub>n-1</sub>]<sup>+</sup>. Figures 2(d) and 2(e) show the one-color REMPI spectra obtained by monitoring [naphthol-(H<sub>2</sub>O)<sub>2</sub>]<sup>+</sup> and [naphthol-(H<sub>2</sub>O)<sub>3</sub>]<sup>+</sup> ( $m/z=198$ ), respectively. In these spectra, two bands are observed at 30 677 and 30 578  $\text{cm}^{-1}$ .

Since we did not observe the ion signal at the mass of [naphthol-(H<sub>2</sub>O)<sub>4</sub>]<sup>+</sup> ( $m/z=216$ ), we assigned the bands at 30 677 and 30 578  $\text{cm}^{-1}$  to the 0-0 bands of the *cis*- and *trans*-2-naphthol-(H<sub>2</sub>O)<sub>3</sub> clusters, respectively. For the 2-naphthol-(H<sub>2</sub>O)<sub>2</sub> and 2-naphthol-(H<sub>2</sub>O)<sub>5</sub> clusters, their ion signals were very weak and we could not determine their masses. As will be discussed later, however, their IR spectra in the  $\nu_{\text{OH}}$  region provide the conclusive evidence for the size and the structure. Table I lists observed frequencies of the 0-0 bands of 2-naphthol-(H<sub>2</sub>O)<sub>n=0-3,5</sub>.

As seen in Fig. 1(b), there is a remarkable tendency for the shift of the 0-0 bands of the  $S_1-S_0$  electronic transition, which are common in both isomers. That is, though the 0-0 band of the  $n=1$  cluster shifts to red, those of the clusters with  $n\geq 2$  shift to blue with respect to that of the  $n=1$  cluster. In addition, it is seen that the 0-0 band of the  $n=2$  cluster shows different features from other clusters. The 0-0 band of *trans*-2-naphthol-(H<sub>2</sub>O)<sub>2</sub> is very weak and a progression of low frequency vibration ( $\sim 20\text{ cm}^{-1}$ ) is seen. For *cis*-2-naphthol-(H<sub>2</sub>O)<sub>2</sub> the band is broad and is observed weakly beneath the sharp 0-0 band of *cis*-2-naphthol-(H<sub>2</sub>O)<sub>3</sub>. These spectral features of the  $n=2$  clusters indicate that their stable structures are quite different between  $S_0$  and  $S_1$ . A similar spectral feature was seen in the  $S_1-S_0$  electronic spectrum of phenol-(H<sub>2</sub>O)<sub>n</sub>.<sup>26</sup>

## B. IR spectra of bare 2-naphthol

Figure 3(a) shows the FDIR spectra of the OH stretching vibrations ( $\nu_{\text{OH}}$ ) of bare 2-naphthol. When the UV frequency was tuned to the band at 30 903  $\text{cm}^{-1}$ , the  $\nu_{\text{OH}}$  band was observed at 3654  $\text{cm}^{-1}$ . When the UV frequency was fixed to the band at 30 585  $\text{cm}^{-1}$ , another  $\nu_{\text{OH}}$  band was observed at 3661  $\text{cm}^{-1}$ . Thus, these results show that the two electronic bands belong to the two different isomers and their  $\nu_{\text{OH}}$  frequencies differ from each other by 7  $\text{cm}^{-1}$ . Figure 3(b) shows the IR spectra of the  $\nu_{\text{OH}}$  vibrations obtained by *ab initio* calculations. The calculated  $\nu_{\text{OH}}$  vibrational frequencies were 3654 and 3661  $\text{cm}^{-1}$  for the *cis*- and *trans*-rotamer, respectively. Thus, the frequency of the *cis*-rotamer is lower than that of the *trans*-rotamer by 7  $\text{cm}^{-1}$ , which agrees fairly well with the observed difference of 7  $\text{cm}^{-1}$ . Thus, the assignment of the *cis*- and *trans*-rotamers provided by Johnson and co-workers in the electronic spectra is confirmed. The result represents that observation of  $\nu_{\text{OH}}$ , and simulation of the spectra gives us conclusive evidence for the identification of rotamers.

In the *ab initio* calculations, the energy difference of the zero-point level between the two rotamers was also obtained

TABLE I. Observed frequencies of the 0-0 bands of 2-naphthol-(H<sub>2</sub>O)<sub>n</sub> ( $n=0-5$ ). Also shown are the red-shifts of the 0-0 band from that of bare 2-naphthol.

	Observed frequencies (red-shift from the 0-0 band of bare 2-naphthol)/ $\text{cm}^{-1}$					
	$n=0$	$n=1$	$n=2$	$n=3$	$n=4$	$n=5$
<i>cis</i> -2-naphthol-(H <sub>2</sub> O) <sub>n</sub>	30 903	30 532 (-371)	$\sim 30\,670(\sim 233)^a$	30 677 (-226)	...	...
<i>trans</i> -2-naphthol-(H <sub>2</sub> O) <sub>n</sub>	30 585	30 253 (-332)	30 376 (-109)	30 578 (-7)	...	30 263 (-322)

<sup>a</sup>This value is the frequency at maximum intensity of the broad band due to *cis*-2-naphthol-(H<sub>2</sub>O)<sub>2</sub>.

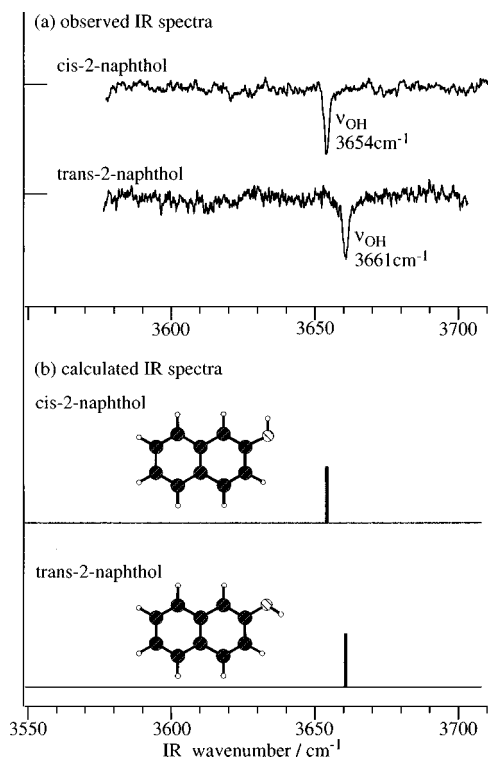


FIG. 3. (a) Fluorescence detected infrared (FDIR) spectra of *cis*- and *trans*-2-naphthol obtained by fixing UV laser frequencies to the bands at 30 903 and 30 585  $\text{cm}^{-1}$ , respectively. (b) IR spectra (stick diagram) of *cis*- and *trans*-2-naphthol obtained by *ab initio* calculation with HF/6-31G basis set.

and the result showed the *cis*-form is more stable than the *trans*-form by 312.5  $\text{cm}^{-1}$ . This result agrees with the study by Schütz and co-workers, who calculated the structures by using the HF/6-31G(*d,p*) basis set.<sup>16</sup> The stable *cis*-rotamer is also confirmed experimentally in the LIF spectrum, in which the intensity of the 0-0 band of *cis*-2-naphthol is three times larger than that of *trans*-2-naphthol. It is known that the thermal population of the isomers is preserved even after the jet expansion, if there exists a substantial potential barrier to isomerization. By using the calculated energy difference, the population ratio of the *cis*- to *trans*-rotamers at 360 K, which is the sample temperature before the expansion, is estimated to be about 3.5. This value is in good agreement with the observed ratio.

### C. IR spectra of 2-naphthol-(H<sub>2</sub>O)<sub>n</sub>

Figures 4(a)–4(f) show the FDIR spectra of the  $\nu_{\text{OH}}$  vibrations of *cis*- and *trans*-2-naphthol-(H<sub>2</sub>O)<sub>n</sub> ( $n=1-3$ ) clusters, which were obtained by fixing the UV laser frequency to the corresponding peaks in Fig. 1(b). The frequencies of the observed vibrational bands are listed in Table II. Also listed are the  $\nu_{\text{OH}}$  frequencies obtained by the *ab initio* calculation. The size dependence of the FDIR spectra of 2-naphthol-(H<sub>2</sub>O)<sub>n</sub> is found to be quite similar to that of phenol-(H<sub>2</sub>O)<sub>n</sub> (see Fig. 3 of Ref. 26). In the following section, we discuss the observed spectra and the structures of each species in detail.

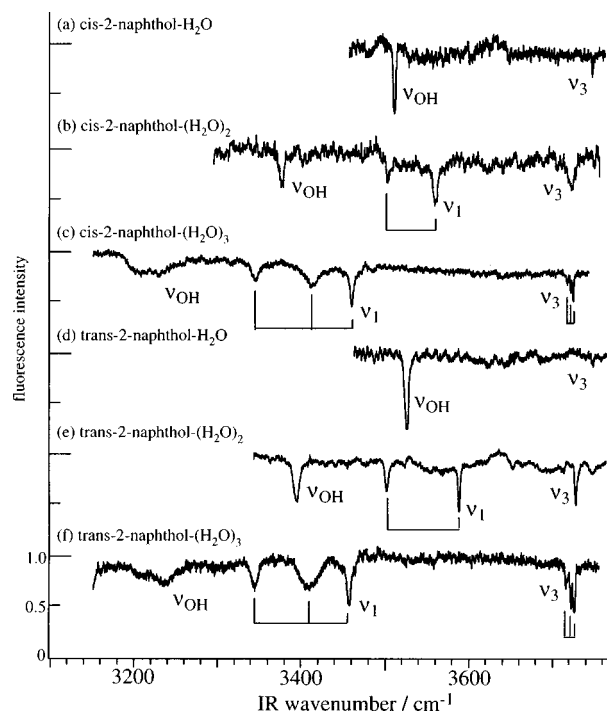


FIG. 4. Fluorescence detected infrared (FDIR) spectra of 2-naphthol-(H<sub>2</sub>O)<sub>n</sub> ( $n=1-3$ ); (a)–(c) *cis*-rotamers, (d)–(f) *trans*-rotamers.

#### 1. *cis*- and *trans*-2-naphthol-H<sub>2</sub>O

Figures 5(a) and 5(b) show the FDIR spectra of *cis*- and *trans*-2-naphthol-H<sub>2</sub>O. Also shown are the spectra of bare 2-naphthol for comparison. The IR spectrum of 2-naphthol-H<sub>2</sub>O shows two  $\nu_{\text{OH}}$  bands at 3512 and 3749  $\text{cm}^{-1}$  for the *cis*-form, and at 3523 and 3748  $\text{cm}^{-1}$  for the *trans*-form. In each rotamer, the intense lower frequency band is assigned to  $\nu_{\text{OH}}$  of the 2-naphthol site, while the higher frequency band is due to the antisymmetric vibration ( $\nu_3$ ) of the H<sub>2</sub>O site. The red-shift of  $\nu_{\text{OH}}$  from that of bare 2-naphthol is 142 and 138  $\text{cm}^{-1}$  for the *cis*- and *trans*-forms, respectively, indicating that the OH bond strength of the 2-naphthol site is reduced by the H-bond formation with H<sub>2</sub>O. In contrast, the  $\nu_3$  band of the H<sub>2</sub>O site is slightly red-shifted from the bare H<sub>2</sub>O molecule (3755.79  $\text{cm}^{-1}$ ),<sup>39</sup> which means that the effect of the H-bond formation on the  $\nu_3$  vibration is very small. This characteristic feature shows that 2-naphthol is acting as a proton donor, and the H<sub>2</sub>O molecule is acting as a proton acceptor. The similar feature of the  $\nu_{\text{OH}}$  bands was also observed in the phenol-H<sub>2</sub>O clusters,<sup>26</sup> whose OH frequencies are also listed in Table II, to be compared with those of the 2-naphthol-(H<sub>2</sub>O)<sub>n</sub> clusters. The observed red-shifts of  $\nu_{\text{OH}}$  of 2-naphthol are slightly larger than those of phenol (133  $\text{cm}^{-1}$ ), corresponding to the larger acidity of 2-naphthol than phenol. Actually, it has been shown that the red-shifts of  $\nu_{\text{OH}}$  of the 1:1 cluster of phenol with various solvent molecules are closely related to the enthalpy changes upon the cluster formation.<sup>27</sup> In this respect, the red-shift is also a measure of acidity of the proton donor. The similar red-shift value of the two rotamers of 2-naphthol indicates that the difference in acidity between *cis*- and *trans*-form is very small. Figures 6(a) and 6(b) show the most stable forms of *cis*- and *trans*-2-naphthol-H<sub>2</sub>O obtained by the *ab initio* calculations, re-

TABLE II. Observed and calculated frequencies ( $\text{cm}^{-1}$ ) of OH stretching vibrations of *cis*- and *trans*-2-naphthol-( $\text{H}_2\text{O}$ )<sub>*n*</sub> (*n*=0–3). Also listed are the vibrations of phenol-( $\text{H}_2\text{O}$ )<sub>*n*</sub> (*n*=0–3) (Ref. 26).

	Observed			Calculated
	Frequency/ $\text{cm}^{-1}$	Assignment	$\Delta \nu_{\text{OH}}/\text{cm}^{-1\text{a}}$	Frequency/ $\text{cm}^{-1\text{b}}$
<i>n</i> =0 ( <i>cis</i> )	naphthol site 3654	$\nu_{\text{OH}}$	...	3654
<i>n</i> =0 ( <i>trans</i> )	naphthol site 3661	$\nu_{\text{OH}}$	...	3661
<i>n</i> =1 ( <i>cis</i> )	H <sub>2</sub> O site 3749	$\nu_3$		3751
	...	$\nu_1$		3615
<i>n</i> =1 ( <i>trans</i> )	naphthol site 3512	$\nu_{\text{OH}}$	-142	3465
	H <sub>2</sub> O site 3748	$\nu_3$		3749
<i>n</i> =2 ( <i>cis</i> )	...	$\nu_1$		3614
	naphthol site 3523	$\nu_{\text{OH}}$	-138	3478
<i>n</i> =2 ( <i>trans</i> )	H <sub>2</sub> O site 3726	$\nu_3$		3729
	...	$\nu_3$		3726
<i>n</i> =3 ( <i>cis</i> )	3560	$\nu_1$		3514
	3503	$\nu_1$		3440
<i>n</i> =3 ( <i>trans</i> )	naphthol site 3376	$\nu_{\text{OH}}$	-278	3336
	H <sub>2</sub> O site 3723	$\nu_3$		3730
<i>n</i> =3 ( <i>cis</i> )	...	$\nu_3$		3724
	3585	$\nu_1$		3509
<i>n</i> =3 ( <i>trans</i> )	3498	$\nu_1$		3434
	naphthol site 3392	$\nu_{\text{OH}}$	-269	3346
<i>n</i> =3 ( <i>cis</i> )	H <sub>2</sub> O site 3722	$\nu_3$		3721
	3719	$\nu_3$		3721
<i>n</i> =3 ( <i>trans</i> )	3715	$\nu_3$		3720
	3458	$\nu_1$		3408
<i>n</i> =3 ( <i>cis</i> )	3411	$\nu_1$		3329
	3343	$\nu_1$		3272
<i>n</i> =3 ( <i>trans</i> )	naphthol site 3226	$\nu_{\text{OH}}$	-428	3174
	H <sub>2</sub> O site 3723	$\nu_3$		3722
<i>n</i> =3 ( <i>cis</i> )	3719	$\nu_3$		3720
	3713	$\nu_3$		3719
<i>n</i> =3 ( <i>trans</i> )	3454	$\nu_1$		3400
	3407	$\nu_1$		3322
<i>n</i> =3 ( <i>cis</i> )	3342	$\nu_1$		3270
	naphthol site 3233	$\nu_{\text{OH}}$	-428	3181
phenol	phenol site 3657	$\nu_{\text{OH}}$	...	3683
phenol-H <sub>2</sub> O	H <sub>2</sub> O site 3748	$\nu_3$		3779
	3650	$\nu_1$		3642
phenol-(H <sub>2</sub> O) <sub>2</sub>	phenol site 3524	$\nu_{\text{OH}}$	-133	3503
	H <sub>2</sub> O site 3725	$\nu_3$		3757
phenol-(H <sub>2</sub> O) <sub>2</sub>	3722	$\nu_3$		3754
	3553	$\nu_1$		3534
phenol-(H <sub>2</sub> O) <sub>2</sub>	3505	$\nu_1$		3463
	phenol site 3388	$\nu_{\text{OH}}$	-269	3369
phenol-(H <sub>2</sub> O) <sub>3</sub>	H <sub>2</sub> O site 3722	$\nu_3$		3750
	3719	$\nu_3$		3749
phenol-(H <sub>2</sub> O) <sub>3</sub>	3715	$\nu_3$		3748
	3451	$\nu_1$		3426
phenol-(H <sub>2</sub> O) <sub>3</sub>	3401	$\nu_1$		3350
	3345	$\nu_1$		3298
phenol-(H <sub>2</sub> O) <sub>3</sub>	phenol site 3236	$\nu_{\text{OH}}$	-421	3208

<sup>a</sup>The red-shift of  $\nu_{\text{OH}}$  from that of monomer.<sup>b</sup>Each frequency is multiplied by a scaling factor of 0.9034.

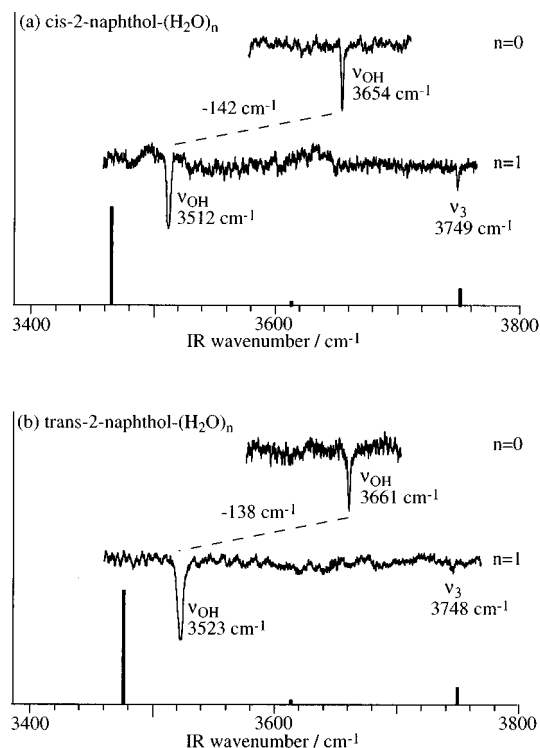


FIG. 5. FDIR spectra and the IR spectra obtained by *ab initio* calculation of (a) *cis*-2-naphthol- $\text{H}_2\text{O}$  and (b) *trans*-2-naphthol- $\text{H}_2\text{O}$ . The FDIR spectra of bare 2-naphthol are also shown for comparison.

spectively. As described above, it is seen that 2-naphthol is acting as a proton donor and  $\text{H}_2\text{O}$  is a proton acceptor. As can be seen in the figure, the clusters have a  $C_s$  symmetry, in which the plane of the  $\text{H}_2\text{O}$  molecule is perpendicular to the plane of the naphthalene ring similar to that of the phenol- $\text{H}_2\text{O}$  cluster. The simulated IR spectra for this form are also shown in Fig. 5 as a stick diagram. A good agreement is seen between the observed and calculated spectra.

## 2. 2-naphthol- $(\text{H}_2\text{O})_n$ , $n=2,3$ ; ring-form structures

*a. 2-naphthol- $(\text{H}_2\text{O})_2$ .* The FDIR spectrum of *cis*-2-naphthol- $(\text{H}_2\text{O})_2$  is shown in the upper part of Fig. 7(a). Four intense bands occur at 3376, 3503, 3560, and 3726  $\text{cm}^{-1}$ . The bands exhibit the characteristic feature of the ring-form cluster similar to the phenol- $(\text{H}_2\text{O})_2$  cluster. In the ring-form cluster, as seen in Fig. 6(c), there are three H-bonded OH oscillators in the ring and two OH oscillators protruding out of the ring. Assuming a local mode picture for the OH vibration, the band at 3376  $\text{cm}^{-1}$  is assigned to  $\nu_{\text{OH}}$  of the 2-naphthol site, and those at 3503 and 3560  $\text{cm}^{-1}$  are assigned to the H-bonded OH oscillators of  $\text{H}_2\text{O}$  molecules in the ring. The band at 3726  $\text{cm}^{-1}$  is assigned to the stretching vibrations of OH groups of  $\text{H}_2\text{O}$  molecules protruding out of the ring, where the two bands are overlapped. The simulated IR spectrum of the ring-form *cis*-2-naphthol- $(\text{H}_2\text{O})_2$  is shown in the lower part of Fig. 7(a). The spectrum was obtained from the energy-optimized ring-form structure, which is shown in Fig. 6(c). The calculated frequencies are also listed in Table II. As can be seen in the figure, the

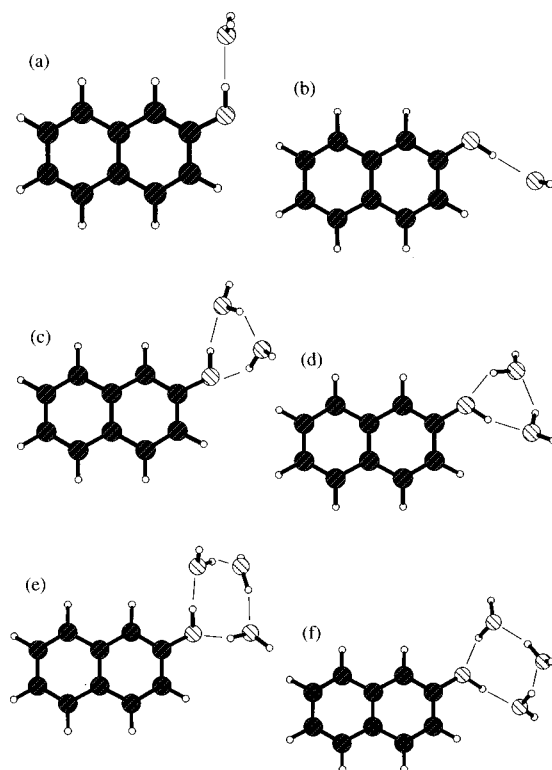


FIG. 6. Structures of 2-naphthol- $(\text{H}_2\text{O})_n$  ( $n=1-3$ ) obtained by *ab initio* calculation. The figures are drawn using the MOLCAT program (Ref. 42).

simulated spectrum reproduces very well the observed one with respect to the frequencies as well as the relative intensities.

Figures 8(a)–8(e) show the vector models of each vibrational mode of *cis*-2-naphthol- $(\text{H}_2\text{O})_2$  with the corresponding harmonic frequencies obtained by the *ab initio* calculations. As seen in the figure, the lowest vibration is assigned to  $\nu_{\text{OH}}$  localized mainly in 2-naphthol. The displacement vectors of the other modes represent more details of the characters of the vibrations; for example, both low frequency OH vibrations of Figs. 8(b) and (c) exhibit in-phase displacements of the two OH oscillators of a  $\text{H}_2\text{O}$  unit, although the amplitudes of the OH oscillations are not symmetry any more. In this respect, these other two modes are assigned to the  $\nu_1$ -type vibrations localized mainly on each  $\text{H}_2\text{O}$  molecule, rather than being assigned as the H-bonded OH oscillators. The higher frequency bands, in contrast, exhibit out-of-phase displacements of the two OH oscillators of the  $\text{H}_2\text{O}$  unit, so that they are called  $\nu_3$ -type vibrations. In this respect, these two modes are also assigned to the  $\nu_3$ -type vibrations of two  $\text{H}_2\text{O}$  molecules, rather than as the OH oscillators free from the ring.

Figure 7(b) shows the observed FDIR and the simulated IR spectra of *trans*-2-naphthol- $(\text{H}_2\text{O})_2$ . Four  $\nu_{\text{OH}}$  bands at 3392, 3498, 3585, and 3723  $\text{cm}^{-1}$  are assigned as  $\nu_{\text{OH}}$  of naphthol site, two  $\nu_1$  of  $\text{H}_2\text{O}$  sites, and  $\nu_3$  of  $\text{H}_2\text{O}$  sites, respectively. It is seen that the spectral features of the clusters of the two rotamers are essentially the same. So, the structure of the *trans*-2-naphthol- $(\text{H}_2\text{O})_2$  cluster is also expected to be the ring form. The lower part of Fig. 7(b) shows the simulated IR spectrum of the energy-optimized ring-form

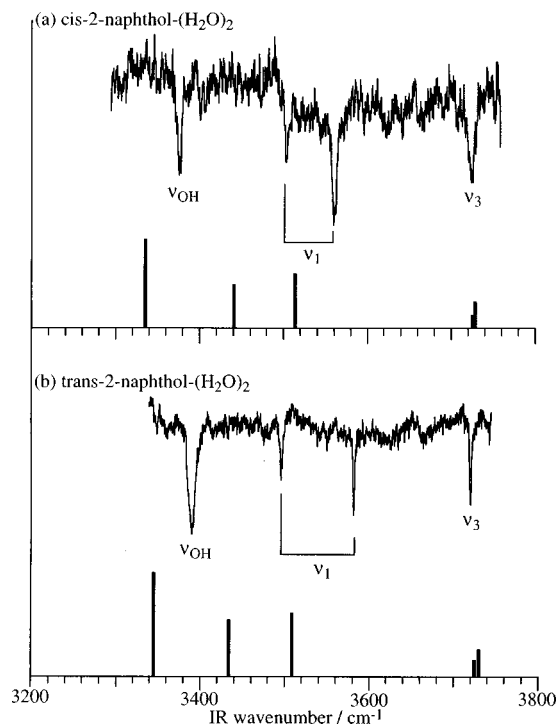


FIG. 7. FDIR spectra and the simulated IR spectra of (a) *cis*-2-naphthol-(H<sub>2</sub>O)<sub>2</sub> and (b) *trans*-2-naphthol-(H<sub>2</sub>O)<sub>2</sub> obtained by *ab initio* calculation.

*trans*-2-naphthol-(H<sub>2</sub>O)<sub>2</sub>. A good agreement is obtained between the observed and the calculated IR spectra, confirming that the structure of *trans*-2-naphthol-(H<sub>2</sub>O)<sub>2</sub> is also of ring form.

Though the vibrational structure is very similar between the two rotamers of 2-naphthol-(H<sub>2</sub>O)<sub>2</sub>, a remarkable difference is seen in the observed spectra shown in Figs. 7(a) and 7(b); the interval of the  $\nu_1$  vibrations of the H<sub>2</sub>O sites is substantially larger in the *trans*-form (b) than that of the *cis*-form (a). Such differences of the OH bands represent the difference in the intermolecular interaction between the clusters of the two rotamers. The 2-naphthol-(H<sub>2</sub>O)<sub>2</sub> cluster is the smallest size ring-form cluster similar to phenol-(H<sub>2</sub>O)<sub>2</sub>

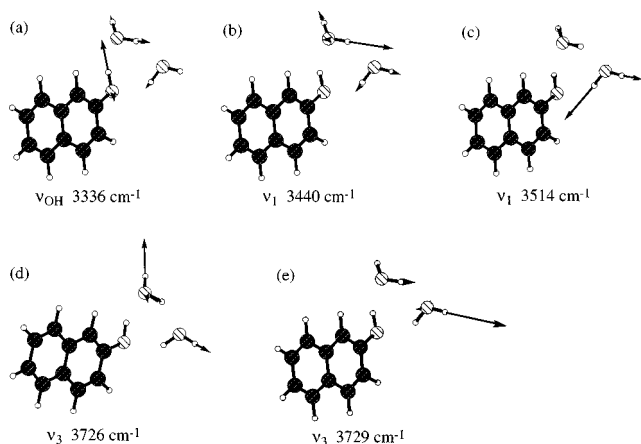


FIG. 8. The vector model of  $\nu_{\text{OH}}$  vibrations of *cis*-2-naphthol-(H<sub>2</sub>O)<sub>2</sub> with corresponding harmonic frequencies: (a)  $\nu_{\text{OH}}$  of naphthol site, (b) and (c)  $\nu_1$  of H<sub>2</sub>O site, (d) and (e)  $\nu_3$  of H<sub>2</sub>O site. These are obtained by *ab initio* calculation, and multiplied by a scaling factor of 0.9034.

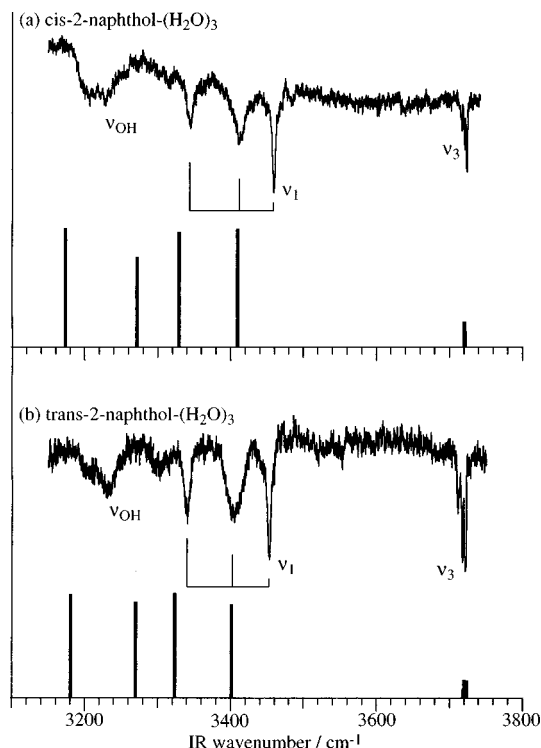


FIG. 9. FDIR spectra and the calculated IR spectra of (a) *cis*-2-naphthol-(H<sub>2</sub>O)<sub>3</sub> and (b) *trans*-2-naphthol-(H<sub>2</sub>O)<sub>3</sub>.

or (phenol)<sub>3</sub>, and it has been pointed out that such a small H-bond ring has a strain in its intermolecular bonds, so that the structure is subject to a balance between the stress and the stabilization by the ring form. The observed differences of the OH bands of the 2-naphthol-(H<sub>2</sub>O)<sub>2</sub>, therefore, seem to be closely related to the balance of the ring formation of both the rotamers. Unfortunately, the simulated spectra by *ab initio* calculation does not reproduce the difference of the band splitting of the  $\nu_1$  vibrations of the H<sub>2</sub>O sites between the two rotamers. From the normal coordinate analysis, it was revealed that the  $\nu_1$  bands at higher energy side ( $\sim 3550$  cm<sup>-1</sup>) are due to those of the H<sub>2</sub>O molecule, which acts as the proton donor to the oxygen atom of the 2-naphthol site. Therefore, the difference in the band splitting of  $\nu_1$  is thought to be due to the difference in the H-bond strength between the oxygen of the OH group of 2-naphthol and the hydrogen of donor H<sub>2</sub>O. Such a rotamer difference may arise from the difference in “through space” interaction between the OH oscillator and the second aromatic ring of 2-naphthol rotamers.

*b. 2-naphthol-(H<sub>2</sub>O)<sub>3</sub>.* The FDIR spectrum of *cis*-2-naphthol-(H<sub>2</sub>O)<sub>3</sub> is shown in the upper part of Fig. 9(a). Seven OH stretching vibrational bands were observed, representing a typical feature of the ring-form cluster. Four of them are lower than 3500 cm<sup>-1</sup> and the remaining three are located close to each other at  $\sim 3720$  cm<sup>-1</sup>. The band at 3226 cm<sup>-1</sup> is assigned to  $\nu_{\text{OH}}$  of the naphthol site, and those at 3343, 3411, and 3458 cm<sup>-1</sup> are assigned to  $\nu_1$  vibrations of the H<sub>2</sub>O molecules in the H-bond ring, that is, H-bonded OH groups of H<sub>2</sub>O. The three bands at  $\sim 3720$  cm<sup>-1</sup> are assigned to  $\nu_3$  vibrations of the three members of H<sub>2</sub>O, which corre-



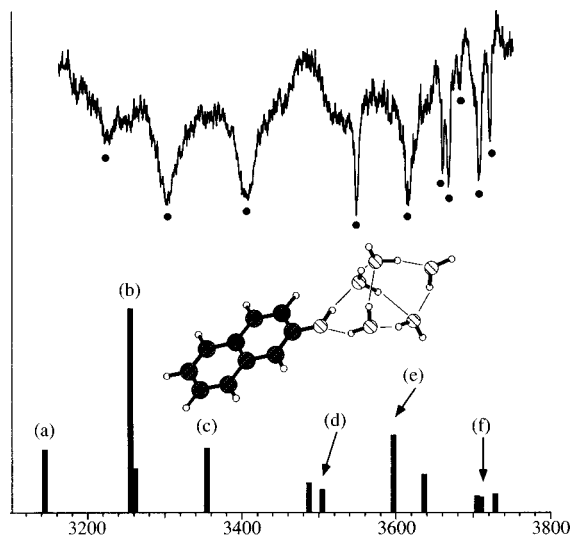


FIG. 10. (upper) FDIR spectrum obtained by tuning UV laser to the band at  $30\,263\text{ cm}^{-1}$  and (lower) the calculated IR spectrum (stick diagram) of 2-naphthol-( $\text{H}_2\text{O}$ )<sub>5</sub> ice (*I*) structure. The observed OH stretching bands are marked by dots. Also shown is the optimized structure of 2-naphthol-( $\text{H}_2\text{O}$ )<sub>5</sub> with ice (*I*) structure.

spond to the OH oscillators protruding out of the ring. There is a large interval between the H-bonded OH band group and the  $\nu_3$  groups, and the interval is called the window region.<sup>26</sup> The stick diagram in the lower part of Fig. 9(a) shows the IR spectra of the energy-optimized ring-form cluster of 2-naphthol-( $\text{H}_2\text{O}$ )<sub>3</sub>, which is shown in Fig. 6(e). It is clear that the simulated IR spectrum of the ring-form structure reproduces well the observed ones. The calculated frequencies are also listed in Table II.

The FDIR spectrum of *trans*-2-naphthol-( $\text{H}_2\text{O}$ )<sub>3</sub> is shown in Fig. 9(b). Seven bands were also observed similar to those of *cis*-rotamer, and the spectral feature of *trans*-rotamer is very similar to that of *cis*-rotamer. Frequencies of these bands are listed in Table II. The lower part of Fig. 9(b) shows the simulated IR spectrum of *trans*-2-naphthol-( $\text{H}_2\text{O}$ )<sub>3</sub>, obtained from the energy-optimized ring-form structure. The calculated spectrum reproduces well the observed one, and it is confirmed that the structure of *trans*-2-naphthol-( $\text{H}_2\text{O}$ )<sub>3</sub> is also of ring-form. Therefore, similar to 2-naphthol-( $\text{H}_2\text{O}$ )<sub>2</sub>, the stable structures of 2-naphthol-( $\text{H}_2\text{O}$ )<sub>3</sub> are of ring-form in both rotamers.

### 3. 2-naphthol-( $\text{H}_2\text{O}$ )<sub>5</sub>; ice (*I*) structure

In the  $S_1-S_0$  LIF spectrum shown in Fig. 1(b), there is an additional band at  $30\,263\text{ cm}^{-1}$ , which is close to the *trans*-2-naphthol- $\text{H}_2\text{O}$  band. Mass-selected MPI spectra did not provide its definite size because of a fragmentation of the cluster after the ionization. So we applied FDIR spectroscopy to this cluster to determine the structure. The upper part of Fig. 10 shows the FDIR spectrum obtained by tuning the UV laser to the band at  $30\,263\text{ cm}^{-1}$ . Seven sharp IR bands occur in the region of  $3500\text{--}3700\text{ cm}^{-1}$ , and three broad bands occur in the region of  $3200\text{--}3400\text{ cm}^{-1}$ . Since the spectrum consists of more than nine  $\nu_{\text{OH}}$  bands, the band at  $30\,263\text{ cm}^{-1}$  in the LIF spectrum is assigned to the cluster with  $n=5$ . As seen in the spectrum, the characteristic feature

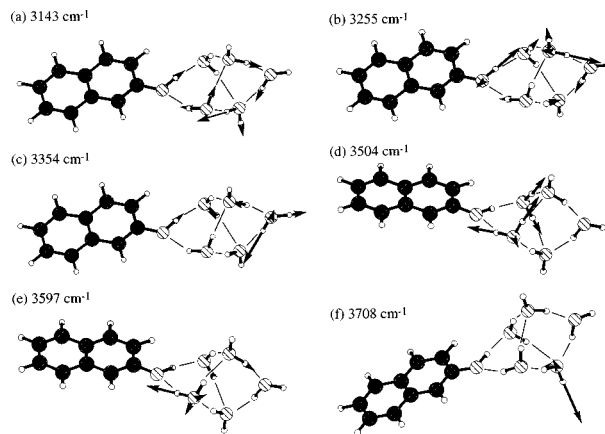


FIG. 11. The vector model of  $\nu_{\text{OH}}$  vibrations of 2-naphthol-( $\text{H}_2\text{O}$ )<sub>5</sub> [ice (*I*)] with corresponding harmonic frequencies (scaled by a factor of 0.9034) obtained by *ab initio* calculation. Each mode corresponds to the band of the simulated IR spectrum in Fig. 10.

is that five  $\nu_{\text{OH}}$  bands are observed between  $3550$  and  $3700\text{ cm}^{-1}$ , that is in the window region. The existence of the  $\nu_{\text{OH}}$  bands in the window region indicates that the structure of this cluster is different from the ring-form structure described above. From the theoretical investigation of phenol-( $\text{H}_2\text{O}$ )<sub>*n*</sub> structures by Watanabe and Iwata, it was demonstrated that the appearance of the OH bands in this region is associated with the presence of one or more  $\text{H}_2\text{O}$  molecules acting as a double proton donor. Especially for the phenol-( $\text{H}_2\text{O}$ )<sub>5</sub>, the IR spectrum of ice (*I*) showed similar vibrational structure with the observed one among the possible isomers whose stabilization energy is within 5 kJ/mol. In the ice (*I*) structure, two  $\text{H}_2\text{O}$  molecules are acting as double proton donors and they exhibit  $\nu_{\text{OH}}$  vibrations in the window region.<sup>31</sup>

In a similar manner, we also calculated the optimized structure of 2-naphthol-( $\text{H}_2\text{O}$ )<sub>5</sub> and compared the calculated IR spectrum with the observed one. In the lower part of Fig. 10 is shown the simulated IR spectra of  $\nu_{\text{OH}}$  vibrations for the optimized ice (*I*) structure of 2-naphthol-( $\text{H}_2\text{O}$ )<sub>5</sub>. Here, we assumed that this cluster belongs to *trans*-rotamer, since the bands of  $S_1-S_0$  transition of this cluster appeared in the *trans*-rotamer region in the LIF spectrum [Fig. 1(b)]. As seen in Fig. 10, the simulated IR spectrum exhibits several bands in the window region, and well reproduces the observed spectrum with respect to the bands in the  $3200\text{--}3400\text{ cm}^{-1}$ . So it is concluded that the band at  $30\,263\text{ cm}^{-1}$  in LIF spectrum [Fig. 1(b)] is due to 2-naphthol-( $\text{H}_2\text{O}$ )<sub>5</sub> and the structure of this cluster is of ice (*I*) type.

Figures 11(a)–11(f) show the vector model of the normal modes for ice (*I*) 2-naphthol-( $\text{H}_2\text{O}$ )<sub>5</sub> obtained by *ab initio* calculations. Each mode corresponds to the bands indicated in the simulated IR spectrum in Fig. 10. As seen in the figure, the bands (a) to (c) mainly involve the  $\nu_{\text{OH}}$  vibrations of naphthol and the  $\text{H}_2\text{O}$  sites. Different from the ring-form structure such as *cis*-2-naphthol-( $\text{H}_2\text{O}$ )<sub>2</sub> shown in Fig. 8, it is seen that the OH stretching vibrations in the region of  $3200\text{--}3400\text{ cm}^{-1}$  are rather delocalized among the OH group of 2-naphthol and five  $\text{H}_2\text{O}$  molecules. The vibrations (d) and (e) are those appearing in the  $3500\text{--}3700\text{ cm}^{-1}$ , that is, in the

window region. The band (d) corresponds to  $\nu_1$  and the band (e) corresponds to  $\nu_3$  of the  $\text{H}_2\text{O}$  molecule, which acts as the double proton donor in the H-bonding network. From these results, it is evident that the bands in the region of 3500–3700  $\text{cm}^{-1}$  in the IR spectrum are due to the existence of “double proton donor  $\text{H}_2\text{O}$  molecules.” The mode (f) corresponds to one of the  $\nu_3$  of three “single proton donor  $\text{H}_2\text{O}$  molecules.”

As to 2-naphthol- $(\text{H}_2\text{O})_4$ , we could not observe the 0-0 band of this cluster in the LIF spectrum. The reason why the band of 2-naphthol- $(\text{H}_2\text{O})_4$  is missing is not clear. The band might not locate in the energy region observed in Fig. 1, or might be broadened by very fast nonradiative process in the  $S_1$  state. The analysis of the electronic spectrum in Fig. 1 is, in that sense, very important in order to characterize the dynamics of the clusters in the  $S_1$  state, which will be the subject of future work.

In summary, the H-bonding structures of 2-naphthol- $(\text{H}_2\text{O})_n$  clusters have been investigated based on the analysis on their OH stretching vibrations. The observations of the OH stretching vibrations of the size-selected clusters could be performed by highly sensitive IR-UV double-resonance spectroscopy. By the comparison between the observed IR spectra with those obtained by *ab initio* calculation, the cluster structures were determined. The stable structures of 2-naphthol- $(\text{H}_2\text{O})_{n=2,3}$  are determined to be of ring form, while that of 2-naphthol- $(\text{H}_2\text{O})_5$ , which is a larger size cluster, is of ice (*I*) form. A similar change of the stable structure from ring to ice with the cluster size is also observed in  $(\text{H}_2\text{O})_n$  and in benzene- $(\text{H}_2\text{O})_n$ .<sup>40,41</sup> Finally, it should also be pointed out that this spectroscopy is also useful in identifying the two rotamers of bare 2-naphthol.

<sup>1</sup>H. Abe, N. Miami, and M. Ito, *J. Phys. Chem.* **86**, 1768 (1982).

<sup>2</sup>A. Oikawa, H. Abe, N. Mikami, and M. Ito, *J. Phys. Chem.* **87**, 5083 (1983).

<sup>3</sup>M. Schütz, T. Bürgi, S. Leutwyler, and T. Fischer, *J. Chem. Phys.* **98**, 3763 (1993).

<sup>4</sup>M. Schmitt, H. Müller, and K. Kleineremanns, *Chem. Phys. Lett.* **218**, 246 (1994).

<sup>5</sup>R. J. Lipert, G. Bermudez, and S. D. Colson, *J. Phys. Chem.* **92**, 3801 (1988).

<sup>6</sup>R. J. Lipert and S. D. Colson, *J. Chem. Phys.* **89**, 4579 (1988).

<sup>7</sup>R. J. Lipert and S. D. Colson, *Chem. Phys. Lett.* **161**, 303 (1989).

<sup>8</sup>R. J. Lipert and S. D. Colson, *J. Phys. Chem.* **94**, 2358 (1990).

<sup>9</sup>T. Ebata, M. Furukawa, T. Suzuki, and M. Ito, *J. Opt. Soc. Am. B* **7**, 1890 (1990).

<sup>10</sup>R. J. Stanley and A. W. Castleman, Jr., *J. Chem. Phys.* **94**, 7744 (1991).

- <sup>11</sup>R. J. Stanley and A. W. Castleman, Jr., *J. Chem. Phys.* **98**, 796 (1993).
- <sup>12</sup>R. Knochenmuss, O. Cheshnovsky, and S. Leutwyler, *Chem. Phys. Lett.* **144**, 317 (1988).
- <sup>13</sup>R. Knochenmuss and S. Leutwyler, *J. Chem. Phys.* **91**, 1268 (1989).
- <sup>14</sup>S. K. Kim, S. Li, and E. R. Bernstein, *J. Chem. Phys.* **95**, 3119 (1991).
- <sup>15</sup>T. Bürgi, T. Droz, and S. Leutwyler, *Chem. Phys. Lett.* **246**, 291 (1995).
- <sup>16</sup>M. Schütz, T. Bürgi, S. Leutwyler, and T. Fischer, *J. Chem. Phys.* **99**, 1469 (1993).
- <sup>17</sup>T. Bürgi, M. Schütz, and S. Leutwyler, *J. Chem. Phys.* **103**, 6350 (1995).
- <sup>18</sup>R. Knochenmuss, G. R. Holtom, and D. Ray, *Chem. Phys. Lett.* **215**, 188 (1993).
- <sup>19</sup>R. D. Knochenmuss and D. E. Smith, *J. Chem. Phys.* **101**, 7327 (1994).
- <sup>20</sup>L. L. Connell, S. M. Ohline, P. W. Joireman, T. C. Corcoran, and P. M. Felker, *J. Chem. Phys.* **94**, 4668 (1991).
- <sup>21</sup>G. Berden, W. L. Meerts, M. Schmitt, and K. Kleineremanns, *J. Chem. Phys.* **104**, 972 (1996).
- <sup>22</sup>G. V. Hartland, B. F. Henson, V. A. Ventura, and P. M. Felker, *J. Phys. Chem.* **96**, 1164 (1992).
- <sup>23</sup>T. Ebata, T. Watanabe, and N. Mikami, *J. Phys. Chem.* **99**, 5761 (1995).
- <sup>24</sup>S. Tanabe, T. Ebata, M. Fujii, and N. Mikami, *Chem. Phys. Lett.* **215**, 347 (1993).
- <sup>25</sup>T. Ebata, N. Mizuochi, T. Watanabe, and N. Mikami, *J. Phys. Chem.* **100**, 546 (1996).
- <sup>26</sup>T. Watanabe, T. Ebata, and N. Mikami, *J. Chem. Phys.* **105**, 408 (1996).
- <sup>27</sup>A. Iwasaki, A. Fujii, T. Watanabe, T. Ebata, and N. Mikami, *J. Phys. Chem.* **100**, 16053 (1996).
- <sup>28</sup>A. Mitsuzuka, A. Fujii, T. Ebata, and N. Mikami, *J. Chem. Phys.* **105**, 2618 (1996).
- <sup>29</sup>R. K. Frost, F. C. Hagemeister, C. A. Arrington, T. S. Zwier, and K. D. Jordan, *J. Chem. Phys.* **105**, 2595 (1996).
- <sup>30</sup>R. K. Frost, F. C. Hagemeister, C. A. Arrington, D. Schleppebach, T. S. Zwier, and K. D. Jordan, *J. Chem. Phys.* **105**, 2605 (1996).
- <sup>31</sup>H. Watanabe and S. Iwata, *J. Chem. Phys.* **105**, 420 (1996).
- <sup>32</sup>N. M. Trieff and B. R. Sundheim, *J. Phys. Chem.* **69**, 2044 (1965).
- <sup>33</sup>J. L. Rosenberg and I. Brinn, *J. Phys. Chem.* **76**, 3558 (1972).
- <sup>34</sup>N. Mikami, I. Suzuki, and A. Okabe, *J. Phys. Chem.* **91**, 5242 (1987).
- <sup>35</sup>M. J. Frisch, G. W. Trucks, M. Head-Gordon, P. M. W. Gill, M. W. Wong, J. B. Foresman, B. G. Johnson, H. B. Schlegel, M. A. Robb, E. S. Replogle, R. Gomperts, J. L. Andres, K. Raghavachari, J. S. Binkley, C. Gonzalez, R. L. Martin, D. J. Fox, D. J. Defrees, J. Baker, J. J. P. Stewart, and J. A. Pople, GAUSSIAN 92, Revision A, Gaussian, Inc., Pittsburgh, PA, 1992.
- <sup>36</sup>A. Oikawa, H. Abe, N. Mikami, and M. Ito, *J. Phys. Chem.* **88**, 5180 (1984).
- <sup>37</sup>J. R. Johnson, K. D. Jordan, D. F. Plusquellic, and D. W. Pratt, *J. Chem. Phys.* **93**, 2258 (1990).
- <sup>38</sup>C. Lakshminarayan, J. M. Smith, and J. L. Knee, *Chem. Phys. Lett.* **182**, 656 (1991).
- <sup>39</sup>G. Herzberg, *Molecular Spectra and Molecular Structures III* (Van Nostrand Reinhold, New York, 1996).
- <sup>40</sup>K. Liu, M. G. Brown, R. J. Saykally, and D. Clary, *Nature (London)* **391**, 591 (1996).
- <sup>41</sup>C. J. Gruenloh, J. R. Carney, C. A. Arrington, T. S. Zwier, S. Y. Fredericks, and K. D. Jordan, *Science* **276**, 1678 (1997).
- <sup>42</sup>Y. Tsutsui and H. Wasada, *Chem. Lett.* 517 (1995).